A miniature sputter deposition chamber for *in situ* film growth studies by synchrotron radiation scattering

N. Schell[1], W. Matz[1,2], W. Neumann[3]
[1] Project Group ESRF-Beamline; [2] Institute of Ion Beam Physics and Materials Research;
[3] Central Department Experimental Facilities and Information Technology
Forschungszentrum Rossendorf, P.O. Box 51 01 19, 01314 Dresden, Germany

J. Bøttiger, J. Chevallier, P. Kringhøj
Institute of Physics and Astronomy, University of Aarhus, 8000 Aarhus C, Denmark

1. Introduction

The technological importance of thin films has stimulated an increasing interest in the detailed characterisation of the structure and morphology of thin films and their interfaces as well as the underlying growth mechanisms. It is a challenge to understand, both experimentally and theoretically, the growth mode and the micro-structural development during deposition of thin films. This development depends crucially on the deposition parameters, and such knowledge is required to tailor the film microstructure for specific applications.

One widespread technique for layer deposition is sputtering. It is applied for pure elements as well as for compounds. As its vacuum requirements are only moderate, electron diffraction as *in situ* characterisation method is not applicable. However, x-rays are in that case a powerful probe. In the literature some deposition chambers for *in situ* x-ray diffraction and reflectivity during sputtering are described [1-4]. They are, however, mostly adapted to a special dedicated instrument and use instrumental functions not commonly available. Our approach was to develop a low cost chamber which allows to follow *in situ* the film growth and post deposition annealing by different modes of synchrotron radiation scattering. The chamber should fit into the standard HUBER six-circle goniometer which is used as a multi-purpose instrument for many other experiments at the materials end-station of the Rossendorf Beamline ROBL in Grenoble [5].

2. Chamber design

In order to get as much information as possible on the growth process, the sputter deposition chamber allows for the following types of experiments:

- symmetric x-ray diffraction (Bragg-Brentano geometry) for measuring out-of-plane lattice constants and texture
- vertical grazing incidence diffraction for enhancing the signal of very thin films and suppressing substrate scattering
- reflectometry for determining the film thickness and interface roughness
- in-plane grazing incidence/exit diffraction (GIXS) for the determination of lattice constants, stress and preferred orientation in the surface plane
- crystal truncation rod scattering to determine the growth mode (*step flow, layer-by-layer* or *island formation*).

To allow the preparation of either multi-component films or multi-layer structures, the chamber is equipped with two magnetrons and inlets for two sputter gases. To start with clean i.e. defined conditions, the vacuum reaches a base pressure of less than 10^{-6} mbar before starting the sputtering process. Furthermore, substrate heating and bias are installed.

Costs aside, the main limitations in the design were geometrical ones. It was necessary to respect the maximum load (15 kg) and space restrictions of the existing standard HUBER goniometer in order to guarantee the high precision of the settings (0.001°) [6]. Taking those

limitations into account one can use all existing installations/equipment at the goniometer like detectors, slits, collimators, filter units without any further modifications. The goniometer itself allows horizontal as well as vertical scattering geometries, and thereby all scattering techniques described above.

Fig. 1 shows the sputter deposition chamber inserted for experiments and Fig. 2 an interior cross-section. A detailed description can be found in Ref. [7]. The chamber consists of three separable parts: A central one connected to the φ-circle of the goniometer and equipped with different flanges on the circumference (for pumps, connected via throttle valves, vacuum gauges and a liquid nitrogen trap) and one bigger flange in the bottom which goes through the opening of the φ-circle and connects the demountable substrate carrier to the chamber. The hemispherical top is equipped with four radiation windows (made from 125 µm thick Kapton and sealed with Viton rings), flanges for the two unbalanced magnetrons (commercially available from AJA International [8]) – each placed at a distance of 100 mm from the substrate and tilted 30 degrees away from the substrate normal.

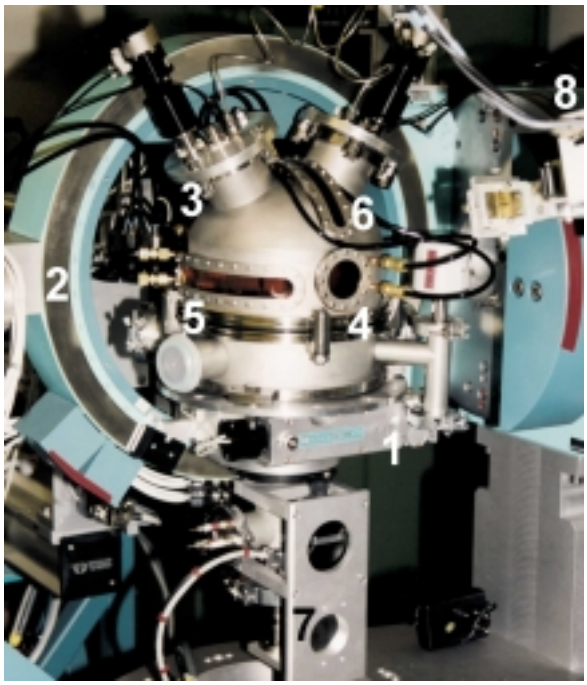

Fig. 1:
Photo of the deposition chamber mounted into the standard Huber six-circle goniometer in the materials end-station of ROBL. 1: φ-circle, 2: χ-circle of Eulerian cradle, 3: magnetrons, 4: beam exit x-ray window, 5, 6: semi-circular large x-ray windows for the diffracted beam in horizontal and vertical planes, respectively, 7: drive for height adjustment of sample, 8: detector unit with slits. The power supply and the gas inlets for both magnetrons come from the top. (The turbo pumps are, however, not yet connected.)

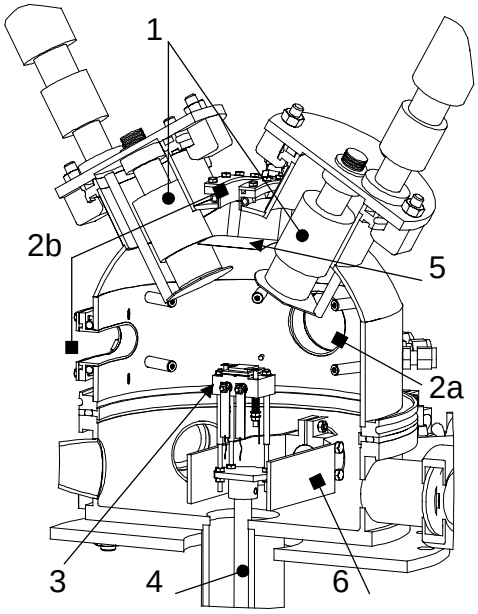

Fig. 2:
Cross section with interior view of the sputter deposition chamber in a central plane. 1: magnetrons with shutters, 2a: entrance window for the incoming beam, 2b: exit windows for the diffracted beams, 3: substrate carrier with heating wires and bias voltage, 4: tube to the z-drive, 5: window protection foils to be fastened at inside protruding bolts, 6: copper disc as liquid nitrogen trap.

All the radiation window flanges are water cooled through outside copper tubes. Additionally, 1 µm thin aluminium foils are mounted on the inner side of the windows in order to protect the Kapton from thermal radiation and contamination by sputtered material. To avoid cross contamination of the two targets, each with a diameter of 1 inch, cylindrical chimneys separate them. Air-pressure-controlled shutters are placed in front of the

chimneys. For each magnetron a sputtering gas inlet is located separately on its corresponding flange.

The substrate (typical size 10x10 mm^2) can be changed by disconnecting only the substrate carrier unit at the bottom flange of the chamber and flooding the chamber with dry nitrogen to minimise contamination of the chamber's inner walls from moisture or oxygen. The BN ceramics substrate holder is mounted on an inside tube connected via a flexible bellow to a precision slide. Driven by an outside stepper motor this allows the sample height to be adjusted by ±7 mm. The electrical feedthroughs for sample heating (resistivity heater up to 650°C), bias voltage and thermocouple are also connected to the substrate carrier unit. The substrate is spring loaded to the BN block by three clamps, one of which is acting as the bias contact. The sample height adjustment and the magnetrons (sputter gas flow, shutter movements) are remote controlled.

The windows limit the angular range for the synchrotron radiation beam. The entrance and exit windows are circular shaped (diameter 40 mm) and asymmetrically arranged (-2^o up to +16°). They are used for reflectometry (total scattering angle usually < 5°) and symmetric wide angle diffraction (total scattering angle < 32°). A second, symmetric, long window in the same vertical plane gives an angular range from 33° to 100° (for wide angle diffraction under grazing incidence). A horizontal window (arranged from -4 mm to +17 mm in respect to the sample horizon) with an opening of 32° to 100° allows in-plane grazing incidence/exit diffraction under maximum grazing angles of 6°.
Despite the angular limitations one can study a large number of substances with widely varying crystal lattice spacings. The tunability of the monochromatic synchrotron radiation wavelength allows for an optimal adaptation to the substance under study.

3. First experiments: texture development in TiN films

After successful trial tests concerning handling and intensity considerations for future typical samples, a question of considerable interest was tackled: the texture development with thickness of TiN films, its manipulation by change of deposition parameters and the identification of the mechanism(s) controlling the crystallographic orientation. In many applications this texture is of paramount importance. The wear resistance of TiN deposited on tools, e.g., depends on the preferred orientation, and with the (111) orientation one gets the largest wear resistance [9]. Frequently, a crossover phenomenon is observed: at small thickness (002) oriented grains (the (002) plane is parallel to the film surface) dominate, while at larger thickness (111) oriented grains take over. In most previous studies [10] the preferred orientation of thin films was explained in terms of surface energy and kinetic factors. In the case of TiN films, it was suggested, that close to equilibrium the (111) grains dominate, while, away from equilibrium, (002) grains dominate.

Pelleg *et al*. [11] have suggested that the thermodynamic driving force for change in orientation of the grains from (002) to (111) in TiN is the difference of the sums of the surface energy and the strain energy of the two types of grains. The strain energy is proportional to the film thickness. The (111) grains have a larger surface energy than the (002) grains and the smaller strain energy. Based on this, they predicted that TiN films will grow with (002) grains at small thickness, where the surface term dominates, while (111) grains appear at larger thickness, because in this state the strain energy dominates. The model did not include details of the mechanism(s) controlling the orientation change of the growing grains. Later, Oh and Je [12] observed experimentally this prediction. But the mechanism for changing the orientation of the growing grains was not described in detail.

By real time synchrotron x-ray scattering, Je *et al.* [13] have studied the preferred orientation of TiN films, deposited by magnetron sputtering and TiN targets (not the usual reactive magnetron sputtering from Ti targets). They observed a crossover thickness, where the dominating growth direction switched from the <002> direction to the <111> and based

their interpretation on the model of Pelleg *et al.* [11]. After change of the growth direction, (002) planes still form the growing surface. However, they were tilted away from the film surface normal, so the (111) planes of the growing grains were parallel with the film surface, and the surface became faceted with a large surface roughness.

In a theoretical paper, Dong and Srolovitz [15] demonstrated that texture may develop by recrystallisation. With computer simulations, they showed that in the case of two neighbouring grains, with different larger defect density (strain energy), the grain boundary migrates. The grain with smaller defect density grew into the other grain. To our knowledge, recrystallisation has not been observed in TiN films.

Experimental studies of the development of the microstructure of TiN films deposited by reactive magnetron sputtering, especially the formation of texture during growth, were performed with the chamber described. The characterisation was done by *in situ* x-ray diffraction and reflectivity in order to determine the dependence on film thickness. Making use of mutual perpendicular scattering geometries allows to determine the orientation of the growing grains. Variable deposition parameters investigated were the depostition temperature (250°C to 450°C) and the bias voltage of the substrate (-30 V or -60 V). Previous RBS measurements have shown that within those parameters stochiometric TiN films can be grown. The annealing behaviour of the growing films was followed by diffraction.

4. Experimental and performance of the sputter chamber

In order to optimise the deposition parameters different TiN films were grown in the chamber. These films were examined with RBS, TEM, and *ex situ* x-ray scattering at a laboratory source. Before deposition the base pressure in the chamber was about $2x10^{-5}$ Pa. The reactive sputter gas was a mixture of Ar (99.9996%) and N_2 (99.99990%) with the ratio 4:1 and a total gas pressure of 0.3 Pa. Only one magnetron was used and run at a dc power of 80 W. The substrates were Si(100) wafers with a 1000 Å amorphous oxide layer on top. For the deposition parameters chosen (bias voltages of -30 V and -60 V and substrate temperatures of 250°C, 350°C and 450°C) the deposition rate was about 1.4 Å/s. The incident x-rays were monochromatised to 12.651 keV (λ = 0.980 Å).

Fig. 3 shows two typical x-ray reflectivity curves recorded *in situ.* Fig. 4 gives the correlation of film thickness with sputtering time for all samples determined from reflectivity, demonstrating the linearity of the sputter deposition with time and the subtle dependence on the corresponding deposition parameters.

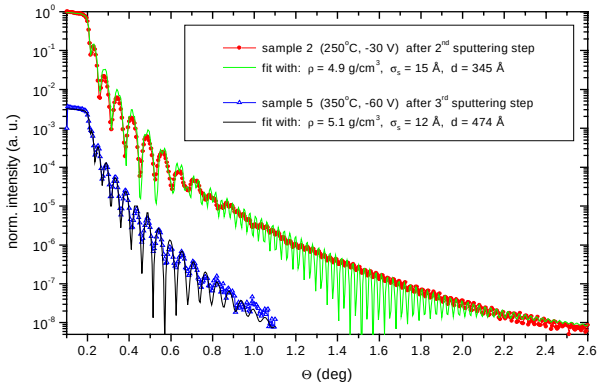

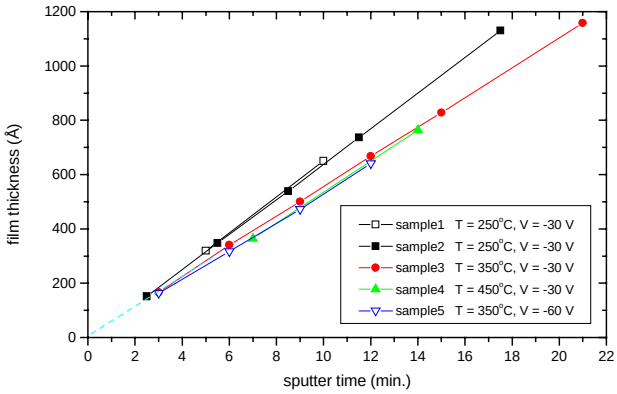

Fig. 3 (left): Typical specular reflectivity data. The upper curve is obtained after the 2nd sputtering step on a film that was deposited at 250°C with a bias voltage of –30 V, and the lower curve is obtained after the 3rd sputtering step on a film that is grown at (350°C; –60 V). The dotted and solid lines are model simulations with the fit values for density, surface roughness and film thickness indicated in the inset.

Fig. 4 (right): Comparison of film thickness against sputtering time for various deposition conditions indicated in the inset.

5. Development of the microstructure and recrystallisation of TiN films

For all chosen parameters the experimental procedure was the same: cleaning by pre-sputtering, sputter deposition for a certain time, interruption of the growth process to characterise the sample by reflectivity (giving density, thickness and roughness of surface and interface), vertical Bragg-Brentano scattering and in-plane (horizontal) GIXS (incidence/exit angles = $0.2^o/0.4^o$, i.e. the x-rays penetrated only approximately 100 Å). The whole process was repeated manyfold. Sometimes several identical scans had been taken to elucidate the temporal (annealing) behaviour (at the elevated deposition temperatures). Sometimes, after film completion, high temperature annealing had been performed. In addition the films had been characterised by TEM. For more details see [16].

Generally, it is found that for all deposition parameters the film growth is characterised by a crossover of the crystallographic orientation of the surface (Figs. 5 and 7) as also seen by other workers [12, 14]. At small film thickness, the (002) grains dominated the vertical diffraction scans while (111) grains took over at larger thickness. Cross sectional TEM micrograph of the TiN films show a columnar structure where the individual columns are composed of grains with low-angle grain boundaries. There is no indication of "competitive growth" in micrographs.

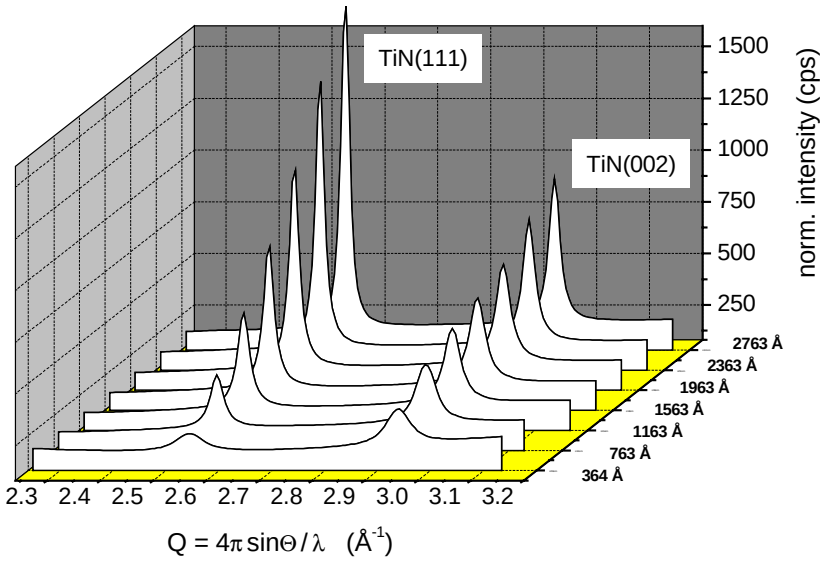

Fig. 5: Three-dimensional representation of a series of vertical Bragg-Brentano diffractograms as a function of film thickness for a film grown at 450^oC with a bias of –30 V. A crossover is clearly seen, with grains having (002) planes parallel with the film surface dominating in the beginning while (111) grains take over at a larger film thickness.

For the first time, however, the underlying mechanism for this texture change could be observed by repeated GIXS scans as demonstrated in Fig. 6. It directly reveals recrystallisation of the topmost layer immediately after deposition. Another proof is the comparison of integrated peak intensities in vertical Bragg-Brentano geometry with those taken by horizontal GIXS scans as demonstrated in Fig. 7: the volume of the (111) grains (their (111) planes are parallel to the film surface) steadily increases with thickness, while the volume of the (002) grains levels off and stays then nearly constant with thickness. This saturation of the volume of the (002) grains stands in contrast to the summed (002) intensity that steadily increases with film thickness, i.e. with each new deposition step. Without recrystallisation (change of crystallographic orientation) of the (002) grains after deposition, the (002) Bragg-Brentano signal should be proportional to the summed (002) horizontal signal, since both signals reflect the volume of (002) grains. The saturation of the (002) signal, therefore, indicates recrystallisation of the (002) grains. Other mechanisms that also influence the texture development – the crossover – cannot be completely excluded. However, mechanisms like the "tilted-(002) surface" [13] and "competitive growth" [14] cannot play a significant role with the present deposition conditions. They should especially

lead to a levelling-off or even decreasing intensity for horizontal-scan (002) diffraction which, however, is in contrast to the actual observations (comp. Fig. 7).

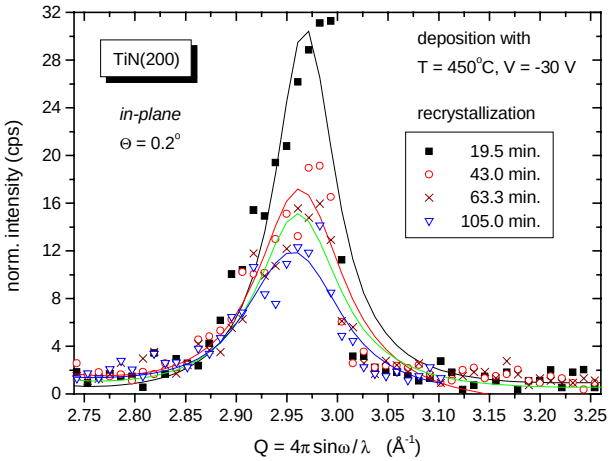

Fig. 6:
TiN(200) horizontal-scan diffraction peaks obtained from a 1963 Å thick film (grown at 450°C with bias –30 V), measured 19.5 min., 43.0 min., 63.3 min. and 105 min., respectively, after the deposition was stopped. The substrate temperature was held constant at 450°C.

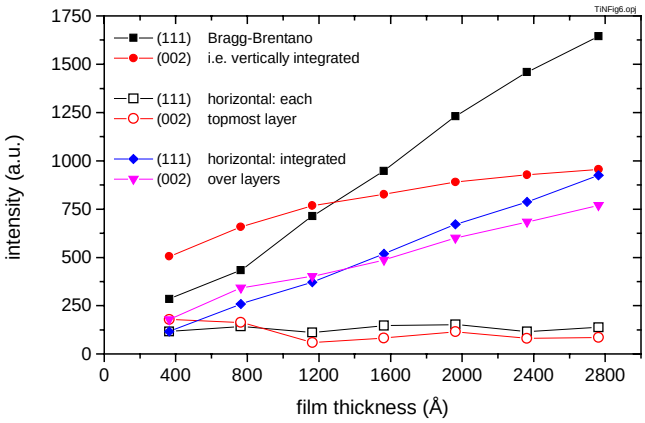

Fig. 7:
Intensity data of the same film as in Fig. 5 (450°C, bias –30 V) shown as a function of thickness. Upper two curves: intensities of the (111) (filled squares) and the (002) (filled circles) Bragg-Brentano diffraction peaks. Lower two curves: intensities of the (111) (open squares) and the (200) (open circles) horizontal-scan diffraction peaks taken under grazing incidence/exit. The two curves in the middle represent the added GIXS intensities – summed up to the corresponding total thickness in question: (111) as filled diamonds and (200) as filled triangles.

The experimental data are consistent with the driving force proposed by Pelleg *et al.* [11]. Assuming this driving force, the crossover thickness increases with decreasing defect density, i.e. lower strain energy. As the defect density decreases with increasing deposition temperature due to defect annealing, the crossover thickness increases with temperature which is indeed observed. During growth, enhancement in the grain size is observed (by TEM micrographs and by a diminishing FWHM of the Bragg peaks with film thickness) which cannot be explained as normal grain growth. Otherwise grain growth/defect annihilation should be observable also during post-annealing. Rather than being thermodynamically driven, the increasing grain size with film thickness is probably controlled by kinetics. As the in-plane lattice constant is smaller than the out-of-plane lattice constant, it is concluded that the films are stressed in compression, with the stress-free lattice parameter lying somewhere between the in-plane and the out-of-plane lattice parameters.

6. Summary

A new, compact sputter deposition chamber which allows for *in situ* study of the growth process by synchrotron x-ray scattering was developed. During growth, the micro-structural development of TiN films – especially the change in texture with film thickness – was studied using *in situ* x-ray reflection and diffraction. Grains with (002) orientation, observed in vertical

diffraction scans, dominate at small film thickness, while (111) grains take over at larger thickness leading to a crossover depending on the deposition parameters. Recrystallisation is identified as a mechanism that controls the development of the texture. The topmost deposited layer has always a significant part of [002] orientation not changing in the deposition process while the lower film parts have already dominating [111] orientation. The recrystallisation of the topmost layer of the film proceeds immediately after the deposition. Post annealung does not change the texture state of the film. The data are consistent with the driving force for the change of orientation of the grains that was suggested by Pelleg *et al.* [11], i.e. the sum of the surface energy and the strain energy of the individual grains was minimised. During growth, the grain size increases with film thickness. This increase is not due to normal grain growth but is probably controlled by the kinetics. As concluded from the measured lattice constants, the films experience compressive stresses.

Acknowledgement

The authors wish to thank I. Heyne, W. Boede, U. Strauch, J. Claußner and A. Bauer for their technical support and assistance during the design and commissioning phase and during the measurements in Grenoble.

References

[1] Hsin-Yi Lee, K.S. Liang, Chih-Hao Lee, and Tai-Bos Wu, J. Mater. Res. **15** (2000) 2606
[2] J.H. Je, D.Y. Noh, H.K. Kim, and K.S. Liang, J. Appl. Phys. **81** (1997) 6126
[3] S. Williams, J.Q. Zheng, M.C. Shih, X.K. Wang, S.J. Lee, E.D. Rippert, S. Maglic, H. Kajiyama, D. Segel, P. Dutta, R.P.H. Chang, J.B. Ketterson, T. Roberts, Y. Lin, R.T. Kampwirth, and K. Gray, J. Appl. Phys. **72** (1992) 4798
[4] J.Q. Zheng, M.C. Shih, X.K. Wang, S. Williams, P. Dutta, R.P. Chang, and J.B. Ketterson, J. Vac. Sci. Technol. A**9** (1991) 128
[5] W. Matz, N. Schell, G. Bernhard, F. Prokert, T. Reich, J. Claußner, W. Oehme, R. Schlenk, S. Dienel, H. Funke, F. Eichhorn, M. Betzl, D. Pröhl, U. Strauch, G. Hüttig, H. Krug, W. Neumann, V. Brendler, P. Reichel, M.A. Denecke, and H. Nitsche, J. Synchr. Rad. **6** (1999) 1076
[6] HUBER X-ray Diffraction Equipment, 83253 Rimsting, Germany
[7] W. Matz, N. Schell, W. Neumann, J. Bøttiger, and J. Chevallier, Rev. Sci. Instrum. (2001) in press
[8] AJA International, P.O. Box 246, 809 Country Way, North Scituate, MA 02060, USA
[9] S. Veprek, Thin Solid Films **130** (1985) 135
[10] M. Kobayashi and Y. Doi, Thin Solid Films **111**, 259 (1984); J.E. Sundgren, Thin solid Films **128**, 21 (1985); J.I. Jeong, J.H. Hong, J.S. Kang, H.J. Shin, and Y.P. Lee, J. Vac. Sci. Technol. A **9**, 261 (1991); D.S. Rickerby, A.M. Jones, and B.A. Bellamy, Surf. Coat. Technol. **37** (1989) 4375
[11] J. Pelleg, L.Z. Zevin, S. Lungo, and N. Croitoru, Thin Solid Films **197** (1991) 117
[12] U.C. Oh and J.H. Je, J. Appl. Phys. **74** (1993) 1692
[13] J.H. Je, D.Y. Noh, H.K. Kim, and K.S. Liang, J. Appl. Phys. **81** (1997) 6126
[14] F. Adibi, I. Petrov, J.E. Greene, L. Hultman, and J.-E. Sundgren, J. Appl. Phys. **73** (1993) 8580
[15] L.Dong and D.J. Srolovitz, Appl. Phys. Lett. **75** (1999) 584
[16] N. Schell, W. Matz, J. Bøttiger, J. Chevallier, and P. Kringhøj, *submitted* to J. Appl. Phys. (2001)